

Article

Resiliency Assessment of Microgrid Systems

Mariam Ibrahim ^{1,*}  and Asma Alkhraibat ²¹ Department of Mechatronics Engineering, German Jordanian University, Amman 11180, Jordan² Department of Computer Engineering, German Jordanian University, Amman 11180, Jordan;
A.Alkhraibat@gju.edu.jo

* Correspondence: mariam.wajdi@gju.edu.jo

Received: 30 January 2020; Accepted: 2 March 2020; Published: 6 March 2020



Abstract: Measuring resiliency of smart grid systems is one of the vital topics towards maintaining a reliable and efficient operation under attacks. This paper introduces a set of factors that are utilized for resiliency quantification of microgrid (MG) systems. The level of resilience (LoR) measure is determined by examining the voltage sag percentage, the level of performance reduction (LoP_R) as measured by percentage of reduction of load served, recovery time (RT), which is the time system takes to detect and recover from an attack/fault, and the time to reach Power Balance state (T_b) during the islanded mode. As an illustrative example, a comparison based on the resiliency level is presented for two topologies of MGs under an attack scenario.

Keywords: microgrid; resiliency metrics; recovery-time; level of performance

1. Introduction

Microgrid (MG) systems have been a topic of interest in the electric power industry worldwide. They effectively integrate a mix of solar, wind, and other Renewable Energy Sources (RES). An MG consists of distributed energy generation units, loads and storage systems interconnected through transmission lines and transformers. It can be operated in two modes, either connected to utility grid mode or islanded mode. In the connected mode, the MG gets energy from its own generation units, but in case of power shortage, power will be provided from the main grid. The surplus power can be sold to the main grid as well. In the islanded mode, the MG operates as an independent power system.

MG can be implemented in different areas, ranging from large buildings to isolated rural villages. Figure 1 presents a diagram of the MG system. The Point of Common Coupling (PCC) is the main Circuit Breaker (CB) that is used to switch the mode of operation between grid-connected and islanded modes. With several roles and purposes supported by MG, many studies have been made, with emphasis on the MG as a promising field of research [1–3]. An overview of the MG system as an essential key in smart energy networks is presented in Reference [4]. Further, an advanced and functional architecture of MG is proposed by Reference [5], with details on obstacles that may face MG, especially during the transition between MG operation modes.

A list of existed MG projects over the globe are given in Reference [6]. For instance, Fort Carson in Colorado Springs is one of several MG projects underway on United States bases under the SPIDERS (Smart Power Infrastructure Demonstration for Energy Reliability and Security) program. The SPIDERS MG is composed of existing assets, a 1 MW PV array and three diesel generators with a total power of 3 MW, and five electric vehicles. The MG project is intended to keep a group of central base facilities operating without grid power as an island, in the event of grid failure. The Sendai MG project was carried out in Japan by New Energy and Industrial Technology Development Organization (NEDO) between 2005 and 2008. The MG showed excellent performance during the 2011 earthquake and tsunami through supplying the teaching hospital of Tohoku Fukushi University with both power and

heat for the duration of the two-day blackout. The MG project in Mannheim-Wallstadt, Germany, was implemented by the state utility company in 2006. The main goal of this project was to develop a true MG able to swiftly and smoothly switch from grid-connected mode to island mode. The system is addressed to residential and commercial units and loads.

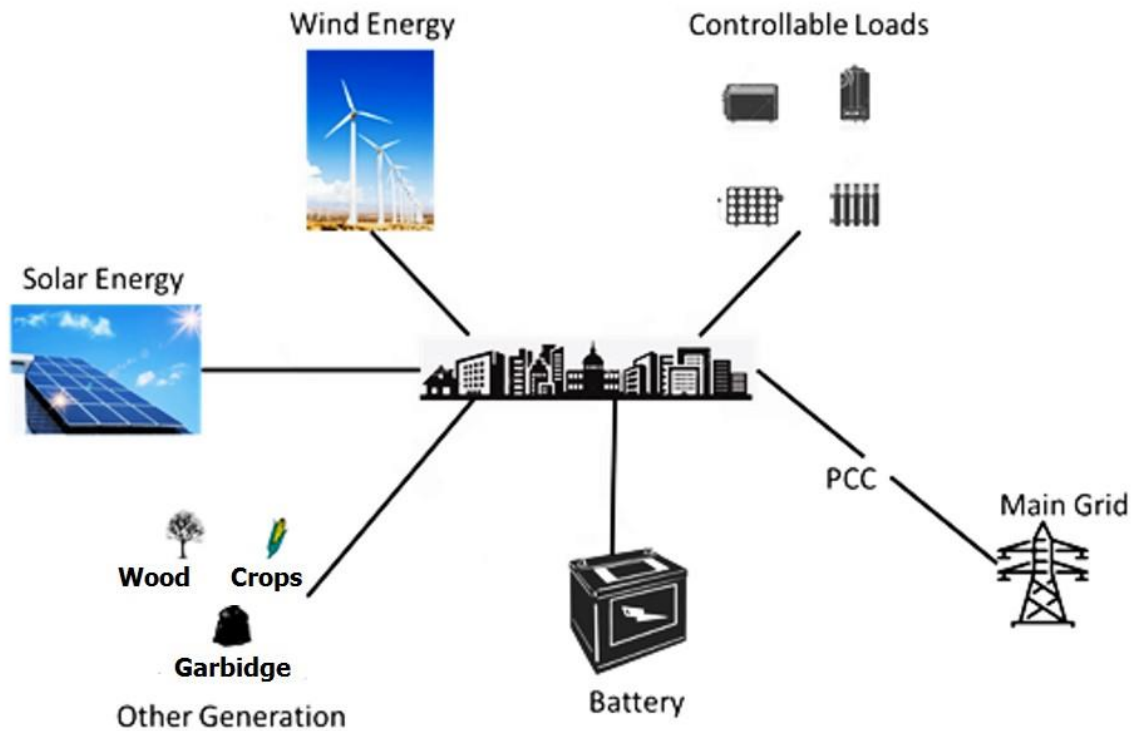


Figure 1. Microgrid system.

Power systems resiliency indicates its capability to cope with the faults and any abnormal conditions that could lead to a power blackout. It also allows recovery of the system in order to retrieve its normal operation. The novelty of this paper lies in introducing the level of resilience (LoR) as a measure to compare and evaluate different MG topologies modeled using MATLAB during a fault/attack scenario. The LoR is determined by the sag voltage percentage, the reduction in load served, and the recovery time. Another merit used in determining the LoR is the time needed to reach the power balance state during the absence of the main grid (islanded mode). In such a mode, we studied the effect of the load shedding technique as a strategy to enhance the resilience of MG under attack. It is shown that the placement of MG resources can affect MG resilience, as given by LoR metric. Thus, using this metric, other designs can be investigated to obtain a best-case resilience using the given set of resources.

The rest of the paper is organized as follows: Section 1.1 presents the latest related work. The topologies and the architecture of the proposed MG are illustrated in Section 2. Section 3 presents the resiliency measure formulation. Section 4 illustrates the resiliency enhancement using Load Shedding technique. Experimental results are shown in Section 5. Section 6 summarizes and presents certain future directions.

1.1. Related Work

Various measures of microgrid (MG) system resilience have been explored in the literature. For instance, Reference [7] presents a method for quantifying the resiliency measure for an MG that is based on networking, Failure rate, and weather factor. In the networking perspective, a connectivity metric is specified by determining the connectivity nature between the installed nodes. Other metrics that have been counted which are the load metric, representing the load that has not been disconnected,

due to emergency cases, such as weather problems. Failure rate indicated the robustness degree of the system, and weather factor defined the weather impacts on the system's resiliency. The blackout duration of the power system is proposed in Reference [8] as a resiliency measure. This outage may occur due to failure in the distribution system. This paper supposed that the resiliency key of the distributed systems is based on two main factors. These factors are the infrastructure of installed power distributed system, and the restoration priority scheme given by the power company. The proposed measure is tested on a residential electrical power distribution system located in part of the City of Phoenix, Arizona. In Reference [9], the authors evaluated the resiliency measure of the MG during high-impact low-probability (HILP) windstorms. This resiliency measure is mainly based on performance reduction and other normalized metrics that are utilized for the resiliency comparison process under different operation conditions. A real MG test-bed is utilized to investigate and examine the proposed methods.

A resiliency quantification technique that mainly aimed to provide a non-interrupted power to the critical load is proposed by Reference [10]. Resiliency estimation is specified as a decision-making problem with multiple measures. It has been quantified through this study by utilizing two approaches, which are: Graph-theoretic approach and Choquet integral. Similar to our work, the simulations of operational contingency scenarios implemented by Reference [10] validate the fact that resiliency of power system depends on the number of paths connecting source units to loads.

An advanced Code-Based Metric is implemented by Reference [11] to quantify the resiliency measure of the power distribution system. This resiliency metric is specified via the simulation process that is based on steady-state and dynamic simulation tools. As shown in the results, the utilization of the output data from the proposed technique highly supported the reliability factor of the system by choosing the suitable design of the power distribution system. Like our work, the scheme presented by Reference [11] can be scalable to different power systems topologies. The concept of Transportable Energy Storage System (TESS) is utilized by Reference [12] during the investigation of the proposed resiliency metric. The authors of this paper proposed a post-disaster recovery scheme that involved the scheduling process of the TESS, and, in turn, generated resources in MGs to meet cost reduction purpose. The proposed recovery scheme is developed as mixed-integer linear programming. An environment of a modified 33-bus test system with three MGs and four TESSs is utilized to test and analyze the proposed model.

The authors of Reference [13] studied the resiliency level of different control systems inside an MG network. They also proposed a Cyber-Physical Resilience Metric (CPRM) that is based on utilizing the vulnerability data to specify the system status for monitoring and management purposes. In order to test the proposed metric and study its impact on resiliency, a case study that is relevant to Ukraine cyber-attack is presented.

In our work, we have reviewed some recent strategies on resiliency enhancement for MGs. For instance, optimal scheduling of microgrid system is developed by Reference [14] to enhance its resiliency. The proposed scheduling procedure is implemented minimizing the load curtailment during the islanded mode operation. It depended on the operations of a centralized control system that is utilized to acquire the needed data and perform the appropriate control commands. It also handled the uncertainty factors of the demand side, generation side, and the transit between operation modes of the MG. The modeling of the normal operation state is achieved via mixed-integer programming. While linear programming is utilized to simulate the resilient operation state. The results of the applied numerical simulation indicated that the proposed model has economic and resiliency merits [15]. Moreover, these results aimed to reduce the required load shedding by developing a new mathematical model based on the survivability factor. The proposed technique is tested on MG during the stand-alone operation mode. The study is built as an optimization problem framework that is considered as a non-linear and non-convex problem. An interior point optimizer (IPOPT) solver is utilized through this study to solve the proposed problem. Results emphasized on the applicability of the proposed system to improve the resiliency of the MG via performing load shedding processes. Analogous to

our scheme [15], specified the load-shedding algorithm based on the load priority aspect. However, they considered a time-dependent priority through the applied algorithm, while we assumed static load priorities.

The authors of Reference [16] proposed an MG system as one of the solutions to meet the common concerns of the power systems. It proposed MG solution as part of an organized resiliency plan to reduce the interruption cases of power to critical loads. It also assessed the implementation of MG as a resiliency key, involving its benefits and technical challenges.

A novel distributed noise-resilient secondary control scheme is proposed by Reference [17]. The proposed control scheme mainly aimed to restore the voltage and frequency parameters. It is implemented on an islanded MG inverter-based with an additive type of noise. Further, the proposed consensus protocols involved both noisy measurements and a non-linear model of the system. MATLAB/SimPowerSystem platform is utilized for simulation purposes to evaluate the performance of the control scheme. Results indicated the effectiveness of the proposed scheme in managing the frequency and voltage parameters and maintaining an accurate proportional real power-sharing.

An algorithm is proposed by Reference [18] to minimize the electrical losses and operational cost. The algorithm is characterized by its resiliency against the communication delay. It also utilized the adaptive step-size that is based on the maximum rate of the imbalance flow. Following numerical simulation of an IEEE 39-bus system, results indicated that the utilization of the adaptive step-size is more efficient than both diminishing static or constant step sizes. Reference [19] developed an MG model that mainly focused on the demand response potentials test. The proposed model aimed to increase the financial gain, and provide a resilient model during the islanded operations. A mathematical technique called Benders decomposition is implemented in order to decompose the model into one master problem and two sub-problems. The master problem optimization is relevant to the status of the generation and battery units. The first sub-problem is based on the optimization of the proposed model operation. The second sub-problem is responsible for the resiliency check of the MG in order to verify safe and reliable operation. The results indicated the effectiveness and economic features of the proposed model.

A new control approach for a Direct Current (DC)-MG is proposed by Reference [20]. An event-triggering communication approach is utilized to provide the data transmission during the inactive status of the Denial of Service (DoS) attack. The stability level of the DC-MG is extracted and derived using both the average dwell-time scheme and the piecewise Lyapunov method.

A resiliency enhancement is covered in Reference [21] by proposing a dynamic MG system that is mainly utilized to recover the installed critical load after abnormal conditions, such as natural disasters. This process is performed using the installed Renewable Energy Resources (RESs), storage systems, and the demand response scheme. The paper also specified the needed budgets to restore the normal operation of the distribution system in case of an emergency.

Unlike the aforementioned works, as far as our knowledge, our work introduces a new framework for determining the resiliency of MG systems. This is done by taking into consideration various aspects as opposed to just one aspect (e.g., the recovery time proposed by References [8,12], and the fraction of load unaffected by distortion used by Reference [11]). Our proposed framework is more general as it includes the aspects of voltage sag percentage, load served, recovery time, and time to reach the power balance state. Furthermore, our framework can allow the improvement of MG scheme as it can provide feedback to the design and development process. In addition to that, References [7,9–11] did not consider enabling resiliency as opposed to our work. In our framework, a resiliency enhancement process is achieved by implementing load-shedding algorithm to meet power balance state. Thus, maintaining the service of critical loads.

2. Microgrid Topology

MG has been previously defined as a small controllable power network that is composed of distributed energy resources, load and transmission systems. A basic formulation scheme of an MG is

presented in Equations (1)–(3). The sets G , D , and SS , represent generation units, demands, and storage systems, respectively. In G , several generation units can be installed in MG. This includes RES (e.g., Photovoltaic (PV), wind), Diesel Generators (DGs), Main grid source, and other units. A classification of the demand side helps in facilitating the calculation and modeling process.

$$G \equiv \{G_{pv}, G_{wind}, G_{DG}, \}$$
 (1)

$$D \equiv \{D_1, D_2, D_3, \dots, D_m\}$$
 (2)

$$SS \equiv \{SS_1, SS_2, SS_3, \dots, SS_n\}$$
 (3)

Each generation system could be classified into several units based on the installation strategy. This classification can be modeled as follow:

$$G_{pv} \equiv \{G_{pv1}, G_{pv2}, \dots, G_{pvi}\}$$
 (4)

$$G_{wind} \equiv \{G_{wind1}, G_{wind2}, \dots, G_{windj}\}$$
 (5)

$$G_{DG} \equiv \{G_{DG1}, G_{DG2}, \dots, G_{DGk}\}$$
 (6)

The classification of the generation, consumption and the storage stages is considered a useful and valuable step, especially during simulation modeling and calculation processes.

For the sake of illustration, we consider a pair of MGs with identical buses, generation and load units, but with different topologies. These topologies are: Bus topology and Ring topology. Figure 2 shows the first microgrid, MG_1 with a bus topology, including three loads and two PV systems. Figure 3 illustrates the ring topology of the second microgrid, MG_2 . Both of the topologies have the same parameters of loads, PV, cables and transformers. The rated voltage of the feeder from the main grid is 11 kV. An 11/0.4 kV transformer is installed between the main grid side and low voltage side. Loads L1, L2, and L3 are connected to buses 4, 5, and 6, respectively. PV1 and PV2 have the rated power of 245 kW for each. The Circuits Breakers (CBs) are utilized in order to meet the fault recovery purpose.

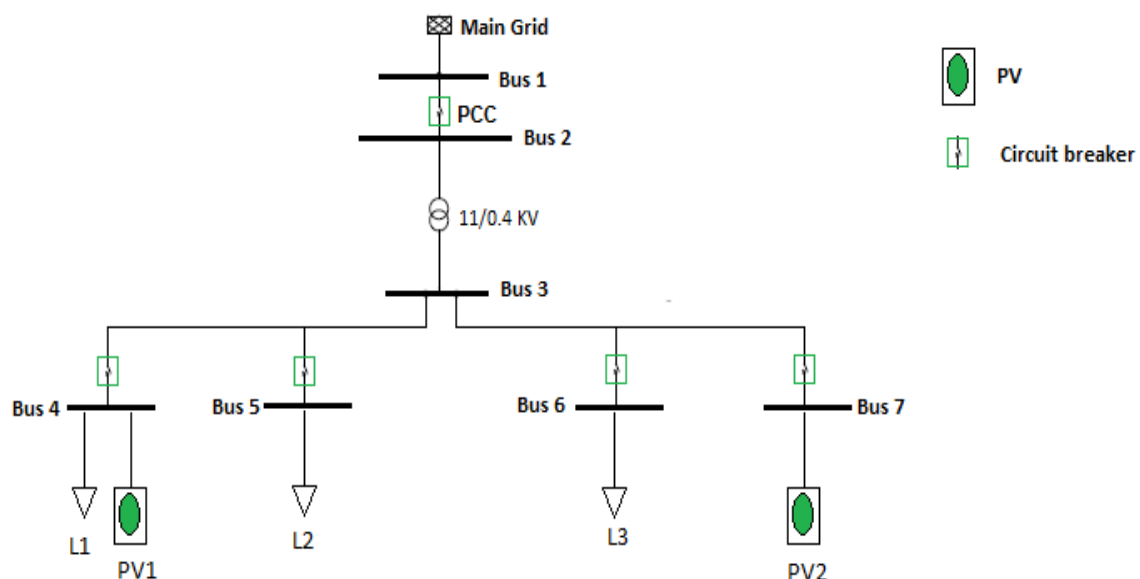


Figure 2. Bus topology of MG_1 .

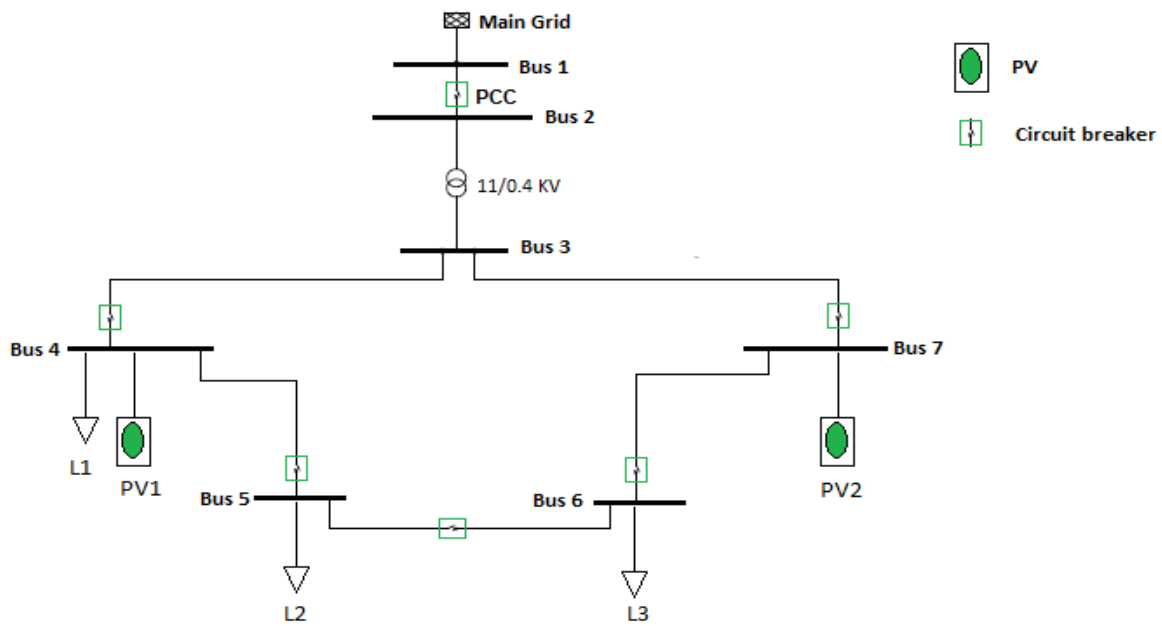


Figure 3. Ring topology of MG₂.

3. Resiliency Measure Formulation

The level of resilience (LoR) is the main factor that will be used to capture the evolution of system parameters through the changes of systems modes of operation under a sequence of fault and recovery actions.

For a number of MGs under a sequence of faults/attacks (fault scenario, F), suppose the resulting system modes are denoted by $N_0 \rightarrow N_1 \rightarrow \dots \rightarrow N_j$, where N_0 is the initial mode, while N_i is the mode after the i th fault and reconfiguration ($i = 1, \dots, j$).

This work investigates a number of factors as a way to compare the resiliency of MGs. These factors are the voltage sag percentage, load served, recovery time, and time to reach power balance state.

Definition 1. Given the sequence of mode switches: $N_0 \rightarrow N_1 \rightarrow \dots \rightarrow N_m$, (under a fault scenario F), the voltage sag [22] can be defined as follow:

$$\text{Sag\%} = \frac{V_0 - V_m}{V_0} \% \tag{7}$$

One of the other vital resilience factors is level of performance reduction (LoP_R). LoP_R is investigated through this study as the load percentage that is served during faults and recovery actions.

Definition 2. Given the sequence of modes: $N_0 \rightarrow N_1 \rightarrow \dots \rightarrow N_m$, (under a fault scenario F), the LoP_R reduction is given by:

$$\text{LoP}_R = \frac{\sum P(\text{loads})I - \sum P(\text{loads})m}{\sum P(\text{loads})I} \% \tag{8}$$

Furthermore, Recovery Time (RT) is considered one of the vital resiliency factors in LoR formulation.

The aforementioned factors have been investigated during the connected mode operation. Regarding the islanded mode, the time to power balance (T_b) factor has been tested. This factor indicates the time needed to meet the power balance state.

Definition 3. Given the sequence of modes: $N_0 \rightarrow N_1 \rightarrow \dots \rightarrow N_m$, T_b can be formulated as:

$$T_b = T|_{P_g \geq P_c} - T_x \tag{9}$$

where, P_g is the generated power, P_c is the consumed power, $t|_{P_g \geq P_c}$ is the time where the generated power is equal or greater than the consumed power. T_x is the time where the MG is operated in the islanded mode.

A system is more resilient if it incurs a smaller sag percentage, or otherwise, a smaller loss of performance, or otherwise a smaller level of recovery-time, or otherwise, a smaller level of time to meet power balance state.

Definition 4. Given a set of microgrids, $MG \equiv \cup MG_k; k \in \{1, \dots, y\}$, where y is the number of the microgrids, and an attack/fault scenario F , we say that $LoR((MG_i, F) > LoR((MG - MG_i, F)$ if:

$$\begin{aligned} & [Sag\% (MG_i, F) < Sag\% (MG - MG_i, F)] \\ \vee & [[Sag\% (MG_i, F) = Sag\% (MG - MG_i, F)] \\ \wedge & [LoP_R (MG_i, F) < LoP_R (MG - MG_i, F)]] \\ \vee & [[Sag\% (MG_i, F) = Sag\% (MG - MG_i, F)] \\ \wedge & [LoP_R (MG_i, F) = LoP_R (MG - MG_i, F)] \\ & \wedge [RT (MG_i, F) < RT (MG - MG_i, F)]] \\ \vee & [[Sag\% (MG_i, F) = Sag\% (MG - MG_i, F)] \\ \wedge & [LoP_R (MG_i, F) = LoP_R (MG - MG_i, F)]] \\ & \wedge [RT (MG_i, F) = RT (MG - MG_i, F)] \\ \wedge & [T_b (MG_i, F) = T_b (MG - MG_i, F)]] \end{aligned}$$

4. Resiliency Enhancement Using Load Shedding

In the islanded mode, we studied the resiliency enhancement using load shedding technique. This technique is mainly based on covering the critical demand in case of the absence of the main grid. Algorithm 1 illustrates the applied scheme. This algorithm starts by continuously sensing the current flowing from the main grid towards the MG. Next, the difference between the generated power and the consumption power, ΔP is computed as given in Equation (10). In general, the power balance state is achieved when the generated power equals the consumed power, as shown in Equations (11) and (12) [23].

$$\Delta P = P_{generated} - P_{consumed} \tag{10}$$

where $P_{generated}$ and $P_{consumed}$ can be given as:

$$P_{generated} = P_{Grid} + P_{PV} + P_{DG} + P_{SS_discharge} \tag{11}$$

$$P_{consumed} = P_{demand} + P_{SS_charge} \tag{12}$$

where P_{Grid} is the power from the main grid, P_{PV} is the PV output power, P_{DG} is the diesel generator power, $P_{SS_discharge}$ is the storage systems power during the discharging, P_{demand} is the demand power, P_{SS_charge} the storage systems power during the charging operation.

Algorithm 1: Load shedding

```

1 Input:  $I_{\text{grid}}, P_{\text{generated}}, P_{\text{consumed}}$ 
2 Output: perform load shedding
3 Start program
4 Sense the  $I_{\text{grid}}$  at PCC
5 If ( $I_{\text{grid}} = 0$ )
6 calculate  $\Delta p$ 
7 endif
8 If  $\Delta P = 0$ 
9 Disconnect noncritical load
10 endif
11 While  $I_{\text{grid}} = 0$  and  $\Delta P < 0$ 
12 perform load shedding
13 End while
14 Stop

```

ΔP has positive, or negative, or zero values. The positive value of the ΔP parameter means that the generated power is more than the demand. In this case, and since there is no storage system in the built-model, other mechanisms can be applied to benefit from this case economically and environmentally. For instance, surplus power can be sold to other organizations, MGs, institutions, etc. On the other hand, if the sign of the ΔP parameter is negative. This means that the demand side is more than the generated power. Other strategies have to be implemented to maintain a stable and reliable operation of the system.

Through this paper, a load shedding algorithm has been implemented to decrease the demand side until the power balance state is achieved. The load shedding algorithm is defined as the process of gradual load disconnection in terms of their serving priorities. In addition to that, the zero value of ΔP indicates the balance state between the generation and the consumption sides. Figure 4 represents the load shedding flowchart. The load shedding is conducted by disconnecting the non-critical loads in ascending order.

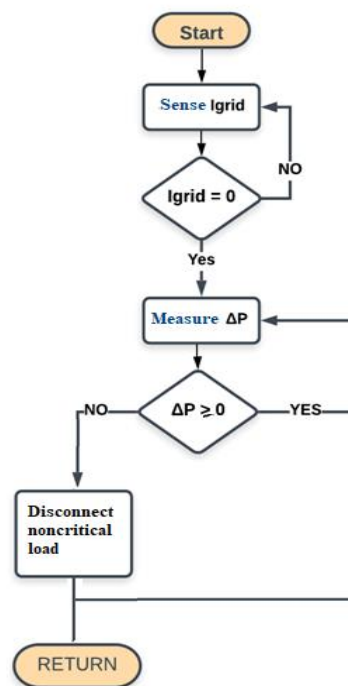


Figure 4. Load shedding flowchart.

5. Experimental Results

The two MGs models are constructed in the MATLAB/Simulink platform version 2018b. Figure 5 shows the MG₁ model, involving the aforementioned MG components. The left side shows the main grid as well as the PCC breaker that connects MG₁ with the utility grid. An 11/0.4 kV transformer is installed between the main grid and the main station. The right side shows the connections between three loads and two PV systems.

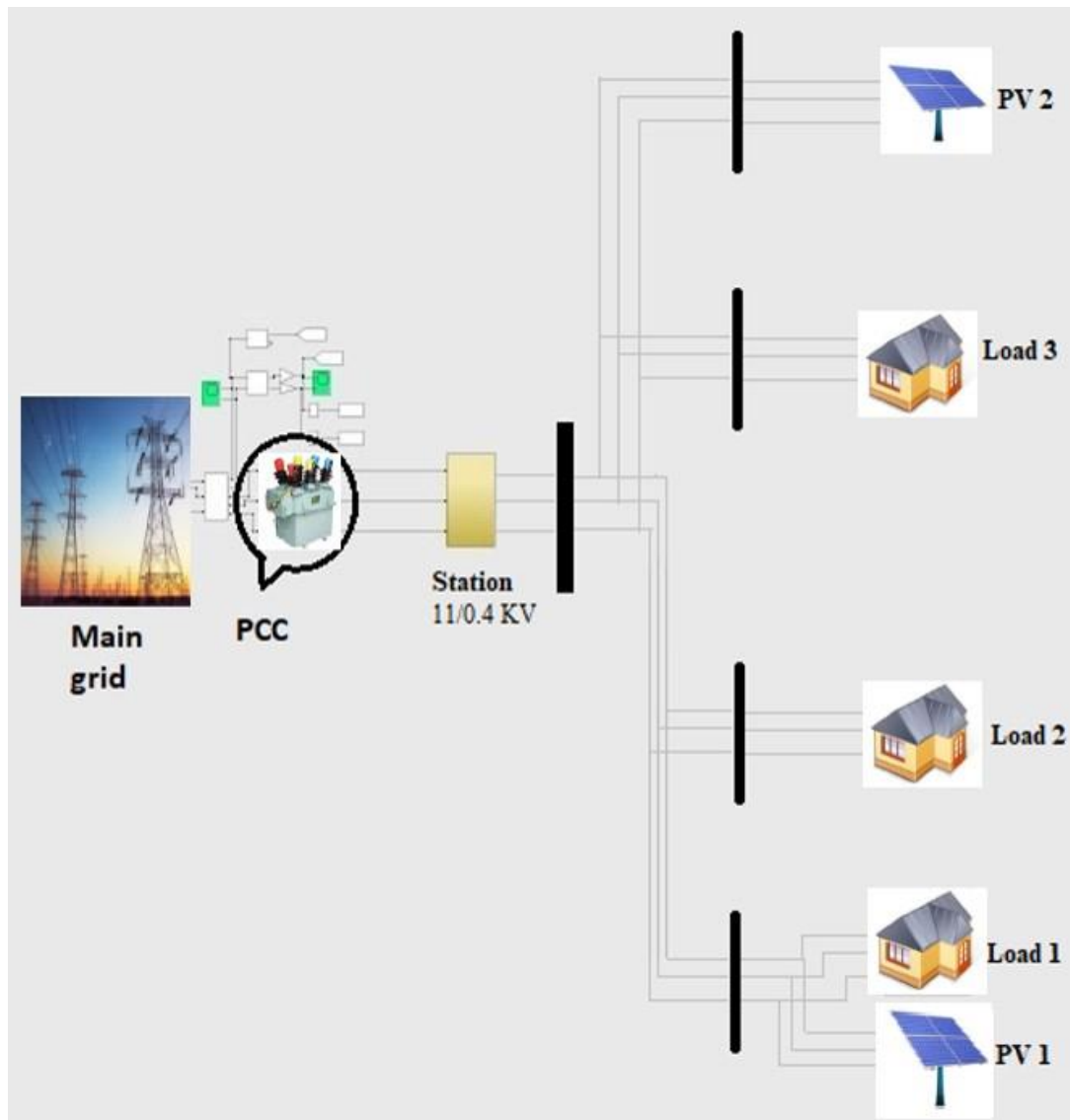


Figure 5. MG₁ model in MATLAB.

Following Algorithm 1, Figure 6a shows the current sensing model of the main grid. In this model, the current signal is monitored continuously and fed into a comparator. If the measured current reaches 0 A, the comparator will trigger the power difference (ΔP) computation phase. Figure 6b shows the computation of ΔP between the generated and the consumed power values. The generated power is the summation of acquired power signals of PV1, PV2, and the main grid, respectively. While the consumed power is the summation of the power signals of L1, L2, and L3, respectively. Both power generated and consumed signals are fed to RMS conversion block in order to calculate the ΔP signal. Figure 6c illustrates the load shedding process in order to meet the power balance state. The process starts by utilizing the ΔP continuously and forwarding it to an Analog to Digital Converter (ADC).

Then, if ΔP value is negative, the non-critical load is disconnected using an ON/OFF signal. For the computation of voltage sag percentage parameter, a voltage signal at the main station is continuously measured and fed to an RMS converter block to extract the RMS values.

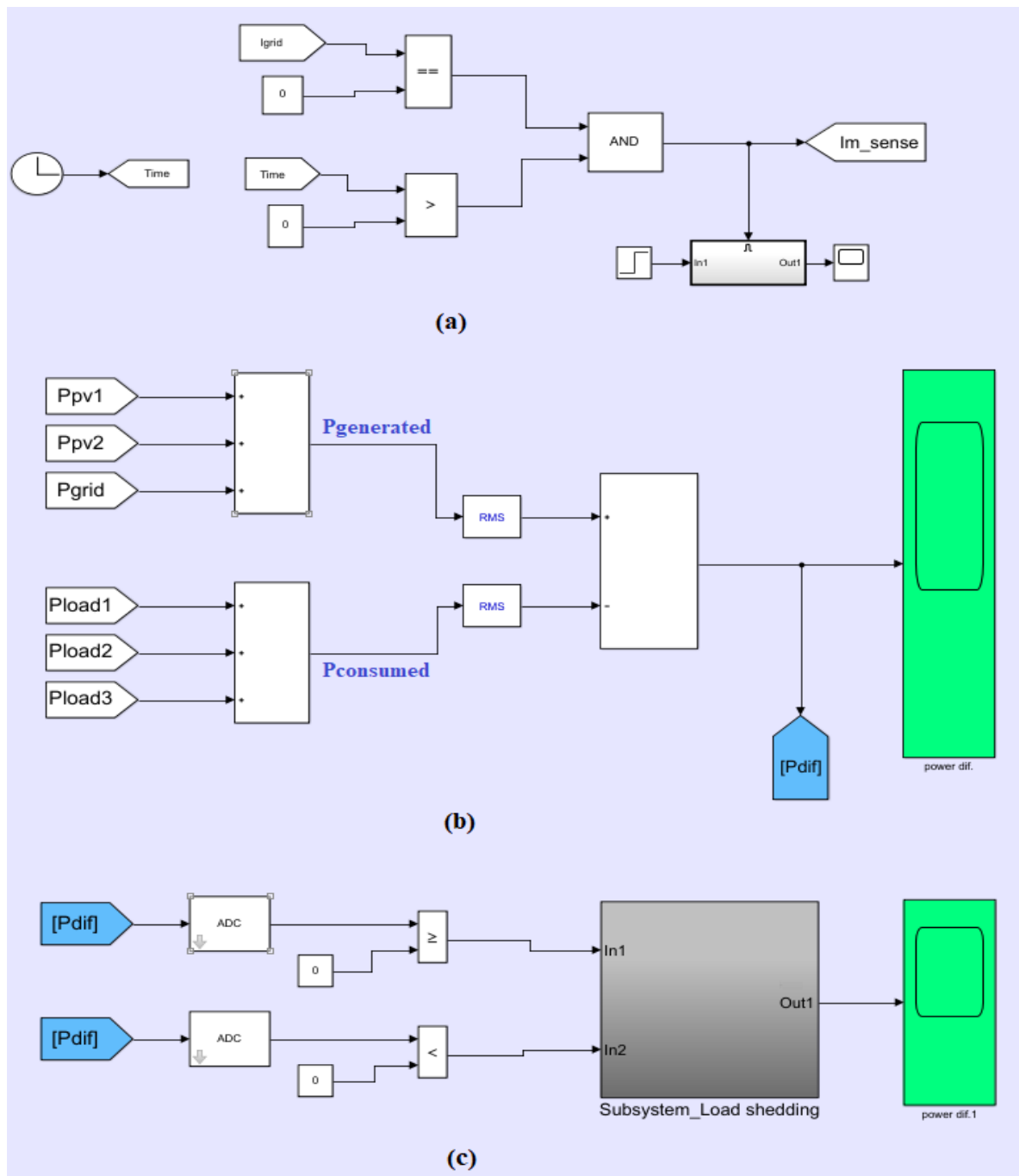


Figure 6. Proposed methods modeling in MATLAB. (a): current sensing model, (b): computation of ΔP , (c): load shedding process.

To evaluate the two MGs factors to different fault types, two faults have been inserted in sequence on different times and at different locations. Fault 1 occurred at bus 5, while fault 2 occurred at bus 1. Generally, electrical faults can be classified into two types, which are: Symmetric faults and Asymmetric faults [24]. Symmetric fault indicates the three-phase fault, which means that all phases are affected by the fault occurrence. The asymmetric fault is called unbalanced fault, which means

that not all the phases are affected by the fault. Typically, asymmetric faults are classified into three types, which are: Line-to-Line (L-L) fault, Line-to-Ground (L-G) fault and Line-to-Line-to-Ground (L-L-G) fault.

The two inserted faults to our models are symmetric fault (fault 1) and asymmetric fault; L-L type (fault 2). As fault 1 is applied at $t = 0.2$ sec at bus 5 and cleared by the simultaneous opening of Circuit Breaker (CB). For MG_1 , this fault has caused a decrease in the voltage parameter from 230 V to 39.7 V at bus 3, as shown in Figure 7a, resulting in a voltage sag of 82.7%. L2 will be disconnected as a result of the fault recovery process. Therefore, and based on Equation (8), the LoP_R is about 31%.

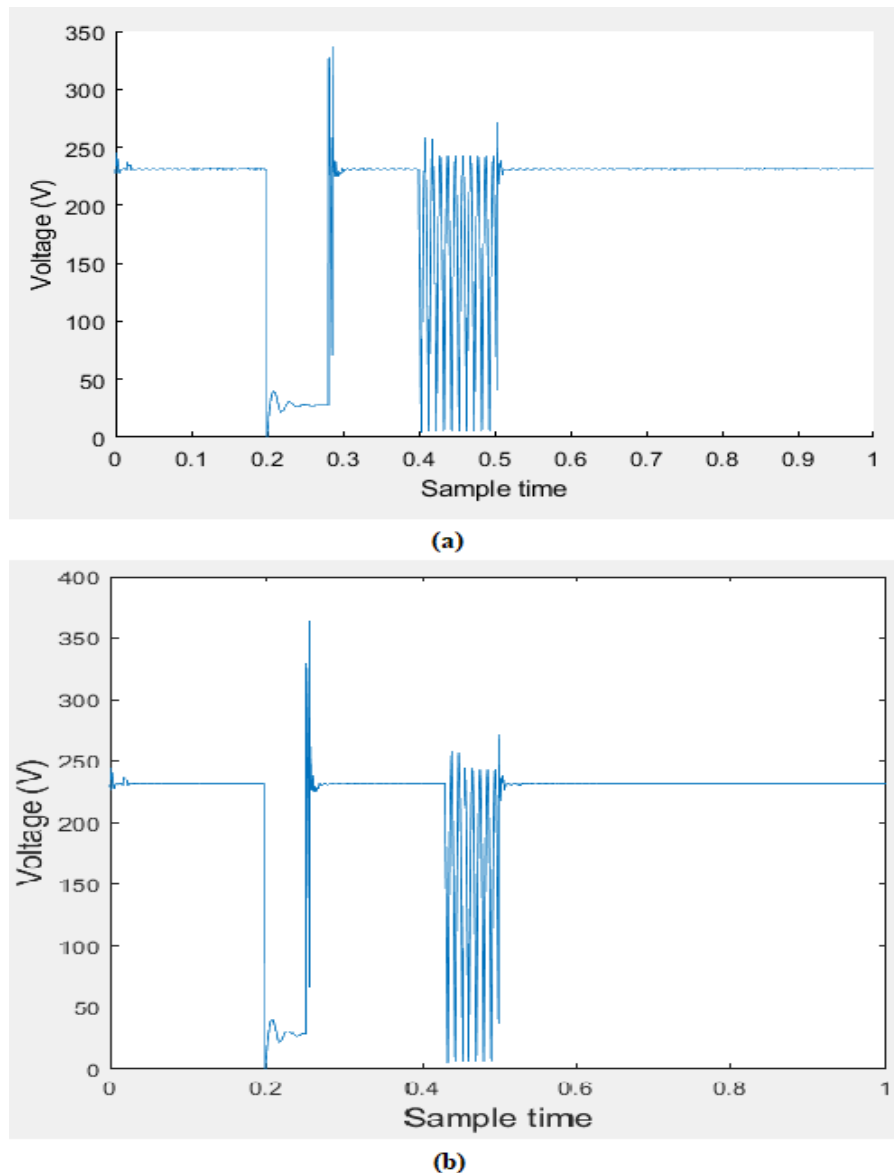


Figure 7. RMS Voltage signal at bus 3: (a) MG_1 , (b) MG_2 .

A second fault is applied at $t = 0.42$ sec at bus 1. This fault has a critical feature which is the location. To maintain the stable operation of MG_1 , the PCC will be opened. Therefore, MG_1 will be transmitted from the connected mode to islanded mode at $t = 0.5$ sec. MG_1 will operate as an independent power source in the islanded mode, as shown in Figure 8. Figure 9a shows the current signal of L2, where the load has been disconnected at about $t = 0.28$ sec as bus 5 is disconnected. The voltage sag parameter has a value of 96%.

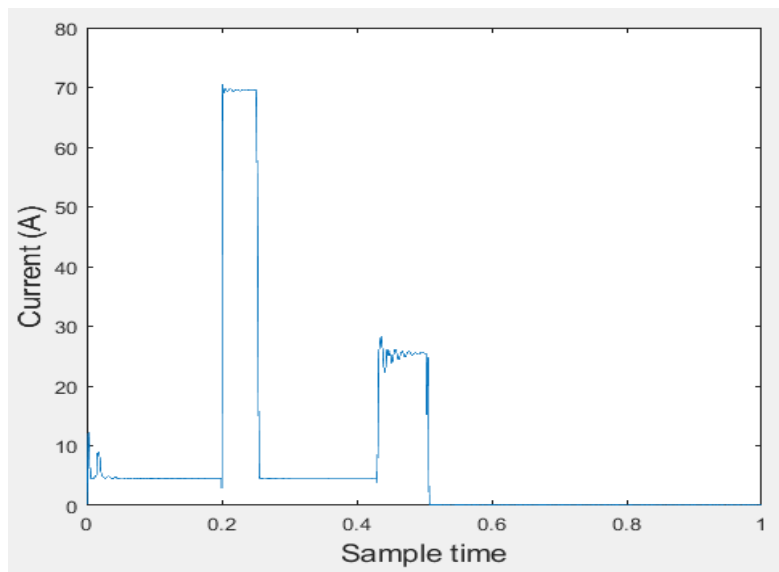


Figure 8. RMS Current signal at the main feeder.

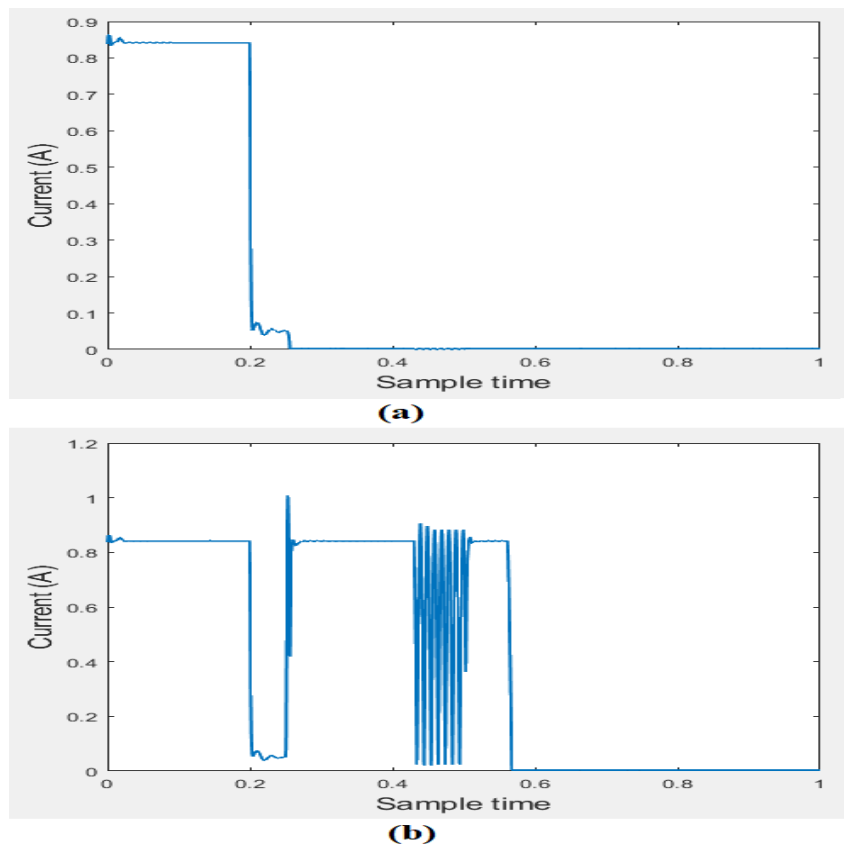


Figure 9. Current signal of L2: (a) MG_1 , (b) MG_2 .

On the contrary, when applying the same sequence of faults for MG_2 , L2 is still connected after fault1 via feeding it with another redundant path through bus 6. Hence, the LoP_R is going to be zero, since there is no load disconnection. The voltage sag values of the MG_2 has approximately the same values of 83% and 96.1% during fault 1 and 2, respectively, as shown in Figure 7b. Under the second fault, fault2, similar to MG_1 , MG_2 will be transmitted to islanded mode at $t = 0.5$ sec. Figure 9b shows the current signal of L2 during the ring topology.

During the islanded mode, maintaining a reliable operation is one of the vital priorities that have to be covered. Therefore, in order to sense the accurate time of the MG transition to islanded mode, a current sensing system is built to sense the current signal of the main grid source. As shown previously in Figure 8, it can be noticed that $T_x = 0.5$ sec for both MG₁, and MG₂.

For both MGs, as the main grid current (I_{grid}) goes to 0 A at $t = 0.5$ sec, the power difference, ΔP is calculated. In this example, L3 is assumed to be the most critical load, while L2 has lower priority than L1 ($Pr_{L2} < Pr_{L1}$), where Pr_{L2} is the priority of L2 and Pr_{L1} is the priority of L1. In MG₁, the gradual load shedding process starts its operation by disconnecting L1, since L2 has been already disconnected during the connected mode. By the load disconnection, ΔP goes to a positive value, and hence, meets the power balance state, as shown in Figure 10a. Following Equation (9), the T_b parameter has the value of 0.06 s. While in MG₂, the load shedding starts by disconnecting L2. The ΔP value is decreased, as shown in Figure 10b; however, it is still negative. Therefore, and based on the proposed algorithm, another disconnection operation of L1 is needed to meet the power balance state. Hence, the T_b parameter has the value of 0.12 s.

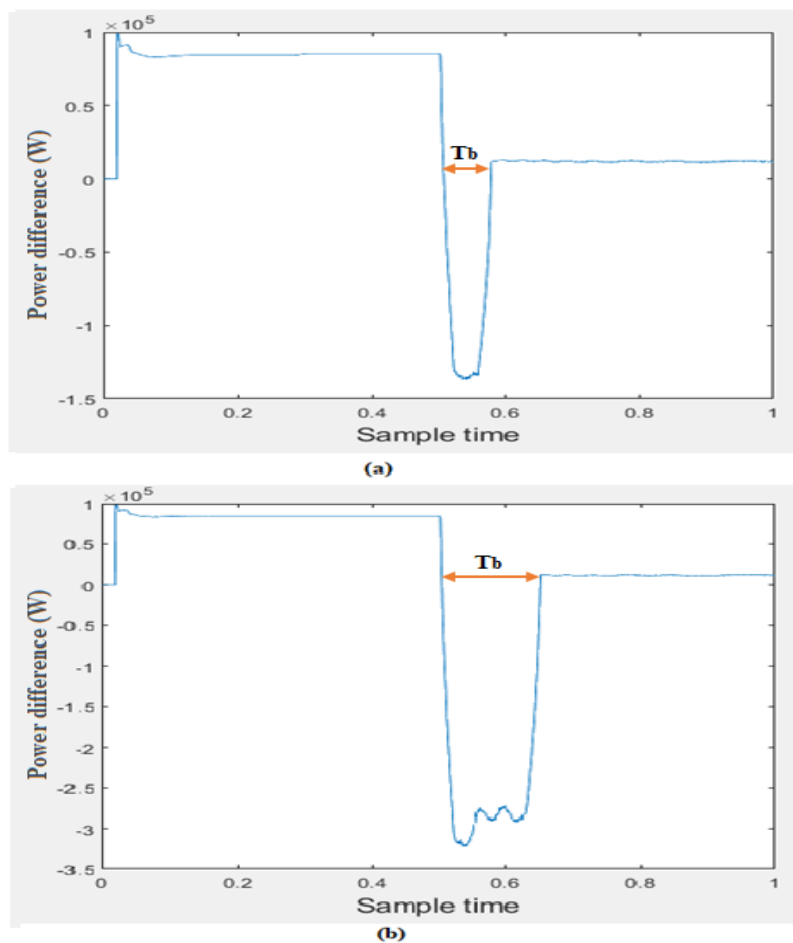


Figure 10. Total power difference, ΔP : (a) MG1, (b) MG2.

Frequency is like the pulse of the power system, and its status indicates the imbalance between generation and real power demand.

Figure 11 illustrates the frequency signals for MG₁ and MG₂, respectively. It can be seen that when the power balance state is reached, the frequency is maintained at its nominal value (50 Hz).

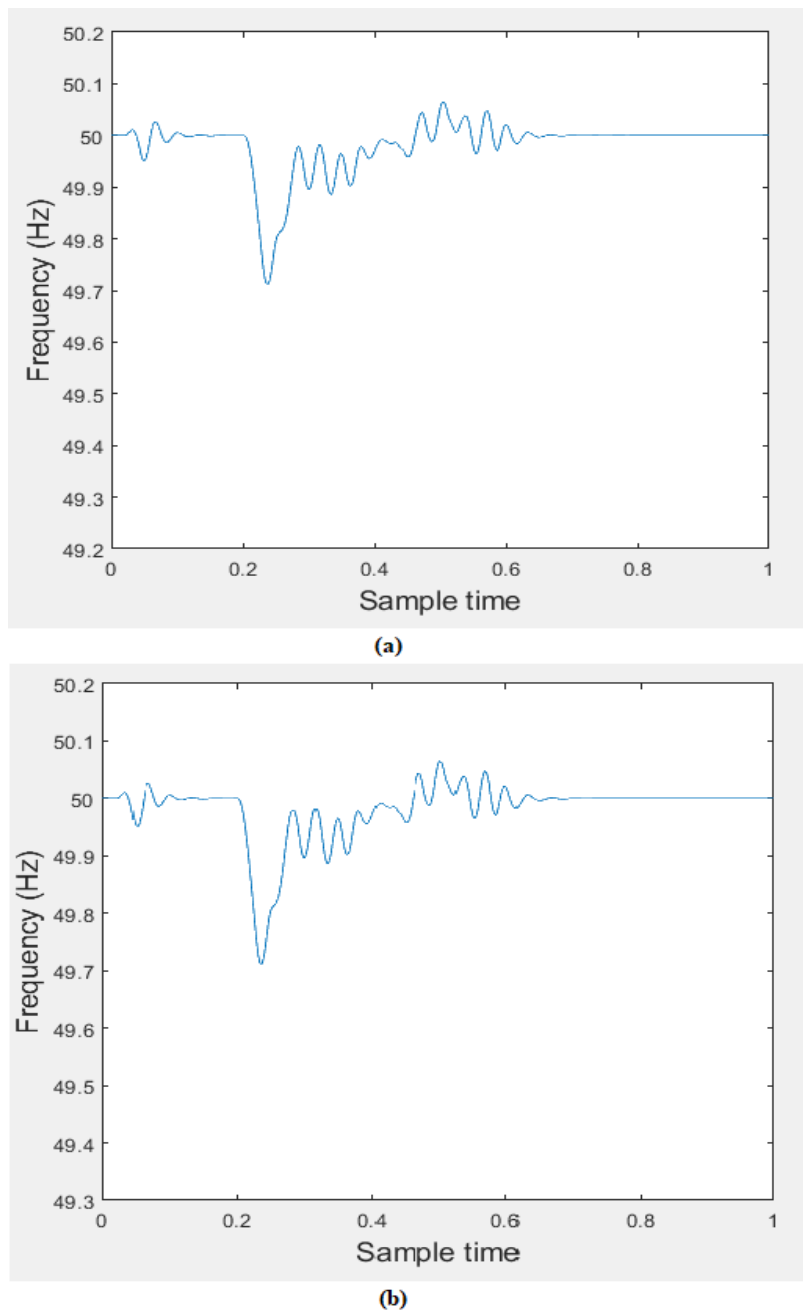


Figure 11. Frequency signal: (a) MG₁, (b) MG₂.

For comparing LoR of MG₁ and MG₂, under a fault scenario F. MG₁ has higher LoP_R (31%) as opposed to MG₂ (0%) during the connected mode. Whereas, both MG₁ and MG₂ have almost the same voltage sag percentage (96%). Then following definition 4, $LoR(MG_2, F) > LoR(MG_1, F)$. Thus, MG₂ is more resilient to fault scenario F as compared to MG₁.

6. Conclusions

This paper proposed a measure for comparing the level of resilience (LoR) for microgrid (MG) systems under attacks/faults. This measure is based on comparing different factors which are: Voltage sag percentage, level of performance reduction (LoP_R), recovery time (RT), in addition to the time to power balance. The LoR of two different MG topologies under a fault scenario is compared. Experimental results showed that, while the two MGs are served by the same generation units and have covered the same set of loads, they have different resiliency levels to the same attack due to

their topological difference. The multi-paths existed in the ring topology of MG₂ allowed serving the loads by the generation side under the given faults with no need to do load disconnection during the connected mode. Therefore, the LoP_R factor has captured the effectiveness of the MG₂ over the MG₁. Regarding the recovery time, which corresponds to the time taken to detect and clear faults, results showed that it does not dramatically vary from one topology to another in which it equals about (0.02–0.04) sec, and so not considered explicitly in the resiliency comparison measure. The time to power balance during the islanded mode is another metric that has been studied in this paper. However, it cannot be directly utilized as a comparison factor, since it has been affected by the load disconnection due to fault recovery decisions. As a future work, evaluating the LoR for more topologies can be tested to choose the best resilience MG design. In addition to that, further development on the resiliency improvement can be achieved via the implementation of deep learning and decision-making concepts to make the MG components more intelligent and allow self-healing features.

Author Contributions: Conceptualization, M.I. and A.A. methodology, M.I. software, A.A. validation, M.I. and A.A. formal analysis, M.I. investigation, M.I. resources, M.I. data curation, M.I. writing—original draft preparation, M.I. and A.A. writing—review and editing, M.I.; visualization, A.A. supervision, M.I. project administration, M.I. funding acquisition, M.I. All authors have read and agreed to the published version of the manuscript.

Funding: This research was funded by Deanship of Graduation Studies and Scientific Research at the German Jordanian University for the seed fund SATS 02/2018.

Conflicts of Interest: The authors declare no conflict of interest.

References

1. Che, L.; Zhang, X.; Shahidepour, M.; Alabdulwahab, A.; Al-Turki, Y. Optimal planning of loop-based microgrid topology. *IEEE Trans. Smart Grid* **2016**, *8*, 1771–1781. [CrossRef]
2. Prete, C.L.; Hobbs, B.F. A cooperative game theoretic analysis of incentives for microgrids in regulated electricity markets. *Applied Energy* **2016**, *169*, 524–541. [CrossRef]
3. Gregoratti, D.; Matamoros, J. Distributed energy trading: The multiple-microgrid case. *IEEE Trans. Ind. Electron.* **2015**, *62*, 2551–2559. [CrossRef]
4. Considine, T.; Cox, W.; Cazalet, E.G. Understanding microgrids as the essential architecture of smart energy. In Proceedings of the Grid-Interop Forum 2012, Irving, TX, USA, 3–6 December 2012; Volume 1, pp. 1–14.
5. Davison, M.J.; Summers, T.J.; Townsend, C.D. A review of the distributed generation landscape, key limitations of traditional microgrid concept & possible solution using an enhanced microgrid architecture. In Proceedings of the 2017 IEEE Southern Power Electronics Conference (SPEC), Puerto Varas, Chile, 4–7 December 2017; pp. 1–6.
6. Examples of Microgrids. Available online: <https://building-microgrid.lbl.gov/examples-microgrids> (accessed on 10 February 2020).
7. Chanda, S.; Srivastava, A.K. Quantifying resiliency of smart power distribution systems with distributed energy resources. In Proceedings of the 2015 IEEE 24th International Symposium on Industrial Electronics (ISIE), Rio de Janeiro, Brazil, 3–5 June 2015; pp. 766–771.
8. Maliszewski, P.; Perrings, C. Factors in the resilience of electrical power distribution infrastructures. *Appl. Geogr.* **2012**, *32*, 668–679. [CrossRef]
9. Amirioun, M.H.; Aminifar, F.; Lesani, H.; Shahidepour, M. Metrics and quantitative framework for assessing microgrid resilience against windstorms. *Int. J. Electr. Power Energy Syst.* **2019**, *104*, 716–723. [CrossRef]
10. Bajpai, P.; Chanda, S.; Srivastava, A.K. A Novel Metric to Quantify and Enable Resilient Distribution System Using Graph Theory and Choquet Integral. *IEEE Trans. Smart Grid* **2016**, *9*, 2918–2929. [CrossRef]
11. Chanda, S.; Srivastava, A.K.; Mohanpurkar, M.; Hovsopian, R. Quantifying Power Distribution System Resiliency Using Code-Based Metric. *IEEE Trans. Ind. Appl.* **2018**, *54*, 3676–3686. [CrossRef]
12. Yao, S.; Wang, P.; Zhao, T. Transportable Energy Storage for More Resilient Distribution Systems with Multiple Microgrids. *IEEE Trans. Smart Grid* **2018**, *10*, 3331–3341. [CrossRef]
13. Venkataramanan, V.; Srivastava, A.; Hahn, A.; Zonouz, S. Enhancing microgrid resiliency against cyber vulnerabilities. In Proceedings of the 2018 IEEE Industry Applications Society Annual Meeting (IAS), Portland, OR, USA, 23–27 September 2018; pp. 1–8.

14. Khodaei, A. Resiliency-Oriented Microgrid Optimal Scheduling. *IEEE Trans. Smart Grid* **2014**, *5*, 1584–1591. [[CrossRef](#)]
15. Balasubramaniam, K.; Saraf, P.; Hadidi, R.; Makram, E. Energy management system for enhanced resiliency of microgrids during islanded operation. *Electr. Power Syst. Res.* **2016**, *137*, 133–141. [[CrossRef](#)]
16. Schneider, K.P.; Tuffner, F.; Elizondo, M.; Liu, C.-C.; Xu, Y.; Ton, D. Evaluating the Feasibility to Use Microgrids as a Resiliency Resource. *IEEE Trans. Smart Grid* **2016**, *8*, 687–696.
17. Dehkordi, N.M.; Baghaee, H.R.; Sadati, N.; Guerrero, J.M. Distributed Noise-Resilient Secondary Voltage and Frequency Control for Islanded Microgrids. *IEEE Trans. Smart Grid* **2018**, *10*, 3780–3790. [[CrossRef](#)]
18. Zholbaryssov, M.; Fooladivanda, D.; Dominguez-Garcia, A.D. Resilient distributed optimal generation dispatch for lossy AC microgrids. *Syst. Control. Lett.* **2019**, *123*, 47–54. [[CrossRef](#)]
19. Dolatnezhad, S.; Amini, M. Enabling demand response potentials for resilient microgrid design. Special Issue on machine learning, data analytics, and advanced optimization techniques in modern power systems. *Sci. Iran. Trans. Comput. Sci. Eng. Electr. Eng.* **2019**, *26*, 3681–3693.
20. Hu, S.; Yuan, P.; Yue, D.; Dou, C.; Cheng, Z.; Zhang, Y. Attack-Resilient Event-Triggered Controller Design of DC Microgrids Under DoS Attacks. *IEEE Trans. Circuits Syst. I Regul. Pap.* **2020**, *67*, 699–710. [[CrossRef](#)]
21. Gilani, M.A.; Kazemi, A.; Ghasemi, M. Distribution system resilience enhancement by microgrid formation considering distributed energy resources. *Energy* **2020**, *191*, 116442. [[CrossRef](#)]
22. Saeed, A.M.; Aleem, S.H.A.; Ibrahim, A.M.; Balci, M.E.; El-Zahab, E.E. Power conditioning using dynamic voltage restorers under different voltage sag types. *J. Adv. Res.* **2016**, *7*, 95–103. [[CrossRef](#)] [[PubMed](#)]
23. Acha, E.; Roncero-Sánchez, P.; De La Villa-Jaen, A.; Castro, L.M.; Kazemtabrizi, B. *VSC-FACTS-HVDC: Analysis, Modelling and Simulation in Power Grids*; John Wiley & Sons: Hoboken, NJ, USA, 2019.
24. Gururajapathy, S.S.; Mokhlis, H.; Illias, H. Fault location and detection techniques in power distribution systems with distributed generation: A review. *Renew. Sustain. Energy Rev.* **2017**, *74*, 949–958. [[CrossRef](#)]



© 2020 by the authors. Licensee MDPI, Basel, Switzerland. This article is an open access article distributed under the terms and conditions of the Creative Commons Attribution (CC BY) license (<http://creativecommons.org/licenses/by/4.0/>).